Int. J. Heat Mass Transfer. Vol. 27, No. 4, pp. 561–571, 1984
Printed in Great Britain

0017–9310/84 $3.00 + 0.00

AN INVESTIGATION OF NATURAL CONVECTION IN ENCLOSURES WITH TWO- AND THREE-DIMENSIONAL PARTITIONS

M. W. NANSTEEL
Department of Mechanical Engineering and Applied Mechanics, University of Pennsylvania, Philadelphia, PA 19104, U.S.A.

and

R. GREIF
Department of Mechanical Engineering, University of California, Berkeley, CA 94720, U.S.A.

(*Received* 19 *October* 1982 *and in revised form* 30 *June* 1983)

Abstract—The heat transfer and fluid flow in a rectangular enclosure fitted with a vertical adiabatic partition is investigated experimentally. The partition is oriented parallel to the two vertical isothermal walls, one of which is heated and the other cooled while all other surfaces of the enclosure are insulated. The experiments are carried out with water for Rayleigh numbers over the range 10^{10}–10^{11} and an aspect ratio (height : width ratio) of one-half. Fluid temperatures are obtained with thermocouple probes and the cross-cavity heat transfer is obtained as a function of the Rayleigh number and partition geometry. The flow is visualized with dye injection. Two cases have been studied. In the first case, the partition is of constant height over the entire breadth of the enclosure resulting in a two-dimensional geometry. The effect of the transverse location and the upward or downward extension (orientation) of the division is examined. In the second case the partition completely divides the enclosure except for a rectangular opening which allows convection to occur across the enclosure. The dependence of the flow and the cross-cavity heat transfer on the Rayleigh number and on the size of the opening in the partition is studied.

NOMENCLATURE

A	aspect ratio, H/L
A_p	aperture ratio, h/H
B	enclosure breadth
b	breadth of opening in partition
c_p	constant pressure specific heat
g	acceleration due to gravity
H	enclosure height
h	height of opening in partition
k	thermal conductivity
k_p	effective thermal conductivity of partition in x-direction
k_p^*	nondimensional partition conductance, $(k_p/k)(L/\Delta x)/Nu_L$
L	enclosure width
Nu_L	Nusselt number, $qL/(T_h - T_c)k$
Pr	Prandtl number, ν/α
Q	heat transfer across enclosure, $(Q_h + Q_c)/2$
q	average heat flux, $Q/(B \cdot H)$
Ra_L	Rayleigh number, $g\beta L^3(T_h - T_c)/\nu\alpha$
T	temperature
T_r	reference temperature, $(T_h + T_c)/2$
u	velocity component in x-direction
v	velocity component in y-direction
x	horizontal position coordinate perpendicular to isothermal walls
x^*	distance separating partition from hot wall
Δx	thickness of partition
y	vertical position coordinate
z	horizontal position coordinate parallel to isothermal walls.

Greek symbols

α	thermal diffusivity
β	coefficient of thermal expansion
θ	dimensionless temperature, $(T - T_c)/(T_h - T_c)$
μ	dynamic viscosity
ν	kinematic viscosity
ρ	density.

Subscripts

c	cold wall
h	hot wall
↑	upward-extending division
↓	downward-extending division.

1. INTRODUCTION

THE PHENOMENA occurring within fluid-filled enclosures with differentially heated sidewalls are of significance in a number of engineering applications. The convective motion which results from buoyant effects arises, for example, in the insulation of a building, in the space between the absorber and cover plates of a solar collector, and in the gas-filled cavity surrounding a nuclear reactor core. A similar although somewhat more complex problem results from the flow of air in passive solar heated buildings. In this context the effect of a vertical partial division on the flow, temperature, and heat transfer at high values of the Rayleigh number is of significant interest. Nansteel and Greif [1] investigated the effect of two-dimensional (2-D) conducting and nonconducting centrally-located partial divisions of various lengths extending vertically downward from the ceiling of a water-filled rectangular enclosure. Results of the flow visualization and vertical temperature profiles were reported along with correlations for the overall cross-cavity heat transfer for

Rayleigh numbers over the range $2.3 \times 10^{10} \leqslant Ra_L \leqslant 1.1 \times 10^{11}$ [1]. Winters [2] used the finite element method to solve for the flow, temperature, and heat transfer in a 2-D, air-filled, rectangular enclosure fitted with a centrally-located division extending upward from the enclosure floor or downward from the ceiling. Calculations were carried out in ref. [2] for Rayleigh numbers over the range 10^4–10^6 and comparisons were made with the data of Duxbury [3]. Good agreement was found in the comparison of ref. [2] for the flow but not for the cross-cavity heat transfer. Chang *et al.* [4] carried out computations for a non-Boussinesq gas in a rectangular enclosure with vertical partial divisions extending upward from the enclosure floor and downward from the ceiling simultaneously. The effect of partition height, thickness and transverse position was examined in ref. [4] for Grashof numbers over the range, 10^3–10^8. Lin and Bejan [5] carried out experimental and analytical investigations for the rectangular enclosure fitted with a vertical partial division similar to the type studied in ref. [1]. The experiments of ref. [5] resulted in heat transfer rates which are considerably larger than those observed in the experiments of ref. [1]. This may be partially due to the smaller aspect ratio ($A = 0.3$) of the enclosure used in ref. [5] ($A = 0.5$ in ref. [1]). The analytical work of ref. [5] consisted of an asymptotic analysis focusing on the limiting regime, $Ra_L \to 0$. The first two terms in the expansion for the stream-function were obtained. Other experimental and numerical investigations for partially divided enclosures include refs. [6–11].

One of the basic problems in passive solar building design is the determination of the energy transfer rate between rooms when a temperature differential exists between walls in adjacent rooms that are connected by a doorway. Geometries of this type result in strong 3-D convection. Investigations in 3-D enclosures are quite limited. Brown and Solvason [12] experimentally and theoretically examined the case of two rectangular compartments that are maintained at different temperatures and are connected by a small opening in a central partition. The relationship between the inter-compartment heat transfer and the driving temperature difference between the compartments was addressed. Weber [13] experimentally studied the temperature field and the heat transfer in a 3-D divided geometry similar to the one investigated here using Freon-12 as the working fluid. Both the height (h) and breadth (b) of the rectangular opening in the partition were varied and the effect on the cross-cavity heat transfer was noted. Weber found that the opening breadth had only a small effect on the heat transfer while the opening height had a substantial effect.

The goal of the present work is two-fold. First, it is desired to experimentally determine, for the case of a 2-D, constant height partition (cf. Fig. 1), the effect of partition orientation (upward or downward extension) and horizontal location for Rayleigh numbers representative of large-scale passive solar applications,

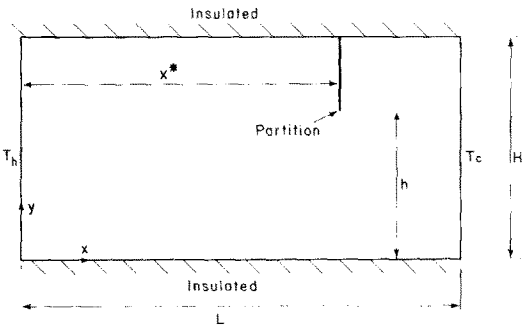

FIG. 1. Sketch of the enclosure fitted with a 2-D partition.

e.g. $Ra_L = O(10^{10}$–$10^{11})$. The case of a downward-extending partition might correspond, for example, to a ceiling beam or 2-D soffit in a room. Experiments are carried out in a water-filled rectangular enclosure of aspect ratio $A = H/L = 1/2$ with isothermal vertical sidewalls and insulated floor, ceiling, and endwalls, cf. Fig. 1. Slender, 2-D partitions of low thermal conductance and height equal to one-half the enclosure height, H, are installed in the enclosure in the downward-extending configuration (↓) at the positions $x^*/L = 1/4$ or $1/2$ or $3/4$ and in the upward-extending configuration (↑) at the center of the enclosure floor, i.e. $x^*/L = 1/2$. Experiments are carried out over the ranges, $3 \leqslant Pr \leqslant 4.5$, $2.25 \times 10^{10} \leqslant Ra_L \leqslant 1.14 \times 10^{11}$. The flow field is visualized by dye-injection and vertical temperature distributions are obtained with thermocouple probes. The dependence of the Nusselt number on the Rayleigh number for the various configurations is presented.

The second configuration studied can be envisioned as the 3-D extension of the case discussed above. The enclosure is divided into two zones of equal volume by a vertical partition of low thermal conductance located in a plane parallel to and midway between the two isothermal walls. The resulting two zones of the enclosure are connected by the single rectangular opening in the division as shown in Fig. 2. The vertical height (h) of the opening is varied between $h = H/4$ and $h = H$ while the opening breadth (b) is maintained constant at $b = L/4 = 0.093B$. Measurements of the cross-cavity heat transfer are carried out over the ranges, $2.4 \times 10^{10} \leqslant Ra_L \leqslant 1.1 \times 10^{11}$, $3.0 \leqslant Pr \leqslant 4.3$. Dye is injected to visualize the basic flow pattern. The heat transfer across the enclosure and the flow behavior are studied for different heights of the rectangular opening. Similarities and dissimilarities with the 2-D partition case, described above, are discussed.

2. EXPERIMENTAL APPARATUS AND PROCEDURE

The experimental apparatus consisted of a rectangular Plexiglas enclosure of height, $H = 15.2$ cm, width, $L = 30.5$ cm, and breadth, $B = 83.8$ cm. The copper hot wall was heated with 18 thermofoil resistance heaters while the cold wall was cooled by

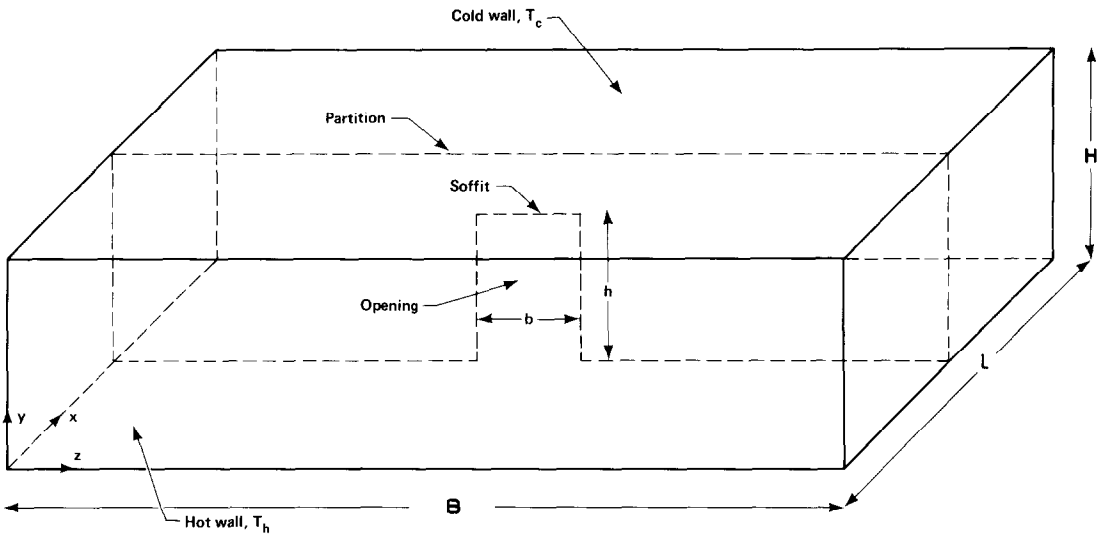

FIG. 2. Sketch of the enclosure fitted with a 3-D partition.

forcing tapwater through two rectangular channels which were milled into the aluminum cold plate, cf. ref. [1]. The maximum deviation from the average wall temperature on the hot and cold walls was kept below 10% of the overall temperature difference ($T_h - T_c$). The average deviation from the mean wall temperature on both the hot and cold walls was about 3% of ($T_h - T_c$). Temperature differences ($T_h - T_c$) ranged from about 25 to 60°C where T_h and T_c are the average temperatures of the hot and cold walls, respectively. The partitions were 9.5 mm thick and were made of polystyrene foam clad with thin sheets of stainless steel. The resulting values for the nondimensional partition conductance, k_p^*, were, $k_p^* \lesssim 0.02$, indicating that heat transfer through the partition represented a very small fraction (2% or less) of the total energy transferred across the enclosure. Thus, most of the heat transfer was due to convection. Hot and cold wall temperatures were monitored with seventeen 30 gauge copper–constantan thermocouples embedded in each wall while the unheated floor and ceiling temperatures were obtained with 50 gauge unsheathed chromel–constantan thermocouples which were cemented to the horizontal Plexiglas surfaces with a thin coat of polyurethane lacquer. Fluid temperatures were measured with 0.25 mm diameter sheathed thermocouple probes which could be moved vertically along the locations $x = L/4$, $x = L/2$ and $x = 3L/4$ in the plane $z = B/2$. Energy input at the hot wall was measured with three wattmeters, each calibrated to an accuracy of about $\pm 1\%$. As a check on the energy losses to the ambient, the heat transfer rate at the cold wall was measured and compared to the power input at the hot wall. Cooling water temperature entering and leaving the cold wall cooling manifold was measured with glass bead thermistors with a calibrated accuracy of ± 0.05°C. At steady state, the maximum difference between the energy input measured at the hot wall, Q_h, and the energy extracted at the cold wall, Q_c, was less than 9% of the total cross-cavity heat transfer.

Due to the finite thermal conductance of the horizontal Plexiglas surfaces, the thermal boundary conditions on the horizontal surfaces of the enclosure were not those of perfectly conducting or perfectly adiabatic surfaces but must have been somewhere in between these two limiting cases. Catton *et al.* [14] have shown that for an enclosure of aspect ratio one-half with $Ra_L = 10^6$ and $Pr \gg 1$ the difference in cross-cavity heat transfer between the perfectly adiabatic and conducting horizontal surface cases is about 20%. For perfectly conducting surfaces the temperature distribution on the enclosure floor is linear, i.e. $(T(x,0) - T_c)/(T_h - T_c) = \theta(x,0) = 1 - x/L$ whereas from Fig. 4 the temperature of the enclosure floor over the range $0.25 \leqslant x/L \leqslant 0.75$ is essentially constant, i.e. $\theta(x,0) \simeq 0.2$. The calculations of Lee and Sernas [15] for air in an enclosure of aspect ratio $A = 0.4$ with adiabatic horizontal surfaces predict floor temperatures in the range $0.2 \lesssim \theta(x,0) \lesssim 0.3$ for $1/4 \leqslant x/L \leqslant 3/4$. Also, Winters' computations [16] for the partially divided water-filled enclosure with $A = 1/2$, $Ra_L = 10^8$ and adiabatic horizontal surfaces show that $\theta(x,0) \simeq 0.2$ in the range $0.25 \leqslant x/L \leqslant 0.75$. It therefore appears from these comparisons that the central portion of the enclosure floor in the present experiment corresponds approximately to an adiabatic surface. This was probably also the case near the vertical walls ($0 \leqslant x/L \leqslant 1/4$, $3/4 \leqslant x/L \leqslant 1$) since cork gasket material was used to thermally isolate the Plexiglas floor from the heated and cooled vertical walls.

Visualization of the flow in the plane $z = B/2$ was accomplished by injecting about 0.5 cm^3 of a dark blue dye into the enclosure at the position $x = L$, $y = H$, $z = B/2$ with a hypodermic syringe. Observation of the subsequent dye motion was made through one of the enclosure endwalls (located in the plane, $z = B$) and was enhanced by a white backdrop at the opposite endwall. The enclosure interior was illuminated by a photographic lamp mounted between the observer and

the endwall observation window. Sketches of the flow pattern are presented. These sketches were generated from numerous experimental observations and adequately characterize the flow phenomena. Further details of the experimental apparatus and procedure can be found in ref. [1].

3. TWO-DIMENSIONAL PARTITIONS: RESULTS AND DISCUSSION

3.1. *Downward-extending partitions*

As discussed in ref. [1], the laminar flow pattern observed in the centrally-divided enclosure in the ↓ configuration is qualitatively independent of Rayleigh number in the range considered and is composed of a peripheral laminar boundary layer, a low velocity internal core region and a weak clockwise recirculation in the upper left-hand quadrant [cf. Fig. 7(a)]. For a non-centrally located division, e.g. $x^*/L = 1/4$ or 3/4, the flow pattern is observed to be qualitatively unaltered. The peripheral laminar boundary layer again separates from the hot wall at approximately the elevation of the lower edge of the partition and crosses the enclosure horizontally in a thin high velocity stream before reattaching to the cool side of the division. Very little if any change in the strength of the clockwise recirculation in the upper left quadrant of the enclosure was noted as partition location was changed. In general, the three flow regions merely change their shape in order to accommodate the varying transverse location of the partition, x^*.

Vertical temperature profiles measured at the positions $x/L = 1/4$, 1/2, and 3/4 for the three transverse partition locations $x^*/L = 1/4$, 1/2, and 3/4 are shown in Figs. 3–5, respectively. Note that these profiles were measured at different values of Rayleigh number; however, meaningful comparisons can still be made because no significant change in the nondimensional temperature field was observed over the range of Rayleigh numbers covered in the present experiments. It should be pointed out that no attempt was made to measure the temperature distribution in the thin

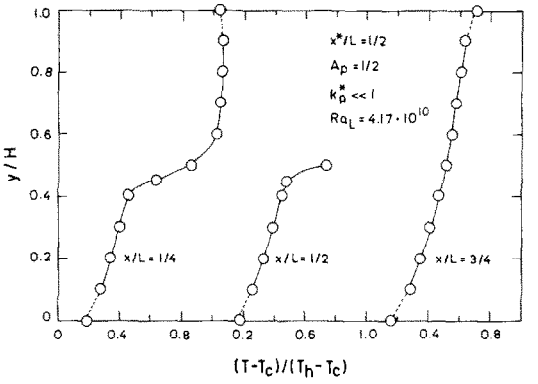

FIG. 4. Vertical temperature profiles with $x^*/L = 1/2$, ↓ configuration, $b/B = 1$.

boundary layers adjacent to the enclosure floor and ceiling. Detailed numerical computations for the case, $A_p = 1$, have shown that for large Ra_L the temperature gradient approaches zero only in a very small region near the surface [17]. Measurements were not made in this region and therefore the data often exhibit an apparent non-zero gradient at $y/H = 0$ and 1. From these figures it is observed that for $x < x^*$, i.e. to the left of the partition, the fluid temperature undergoes a rapid change at an elevation corresponding roughly to the lower edge of the partition, i.e. at $y \simeq h$. At greater elevations ($y \gtrsim h$) the temperature is approximately equal to the hot wall temperature, T_h. Temperatures slightly exceeding the average hot wall temperature T_h are observed in this region because of small nonuniformities in the hot wall temperature (that is, T_h is not the maximum temperature of the enclosure boundary). Also, the small non-zero temperature gradient observed at $y = H$ for $x < x^*$ is probably due to a small conduction heat loss since little convection occurs in this region. For elevations below the division ($y \lesssim h$) the temperature profile appears very similar to the result when no partition is present, i.e. a stable, linear stratification, cf. refs. [1, 18]. The large gradient in temperature at $y \simeq h$ is consistent with the position

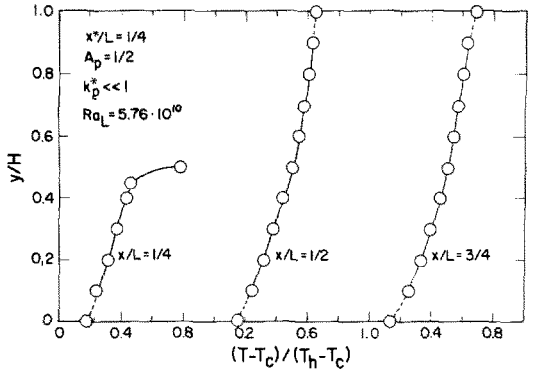

FIG. 3. Vertical temperature profiles with $x^*/L = 1/4$, ↓ configuration, $b/B = 1$.

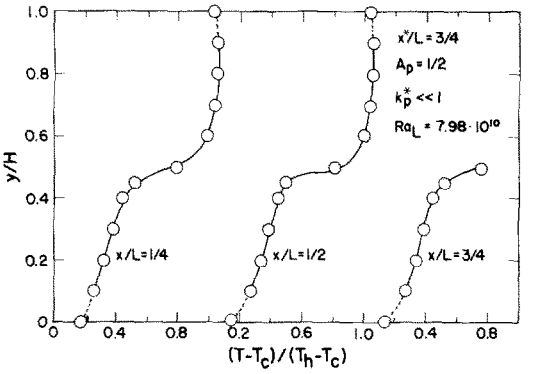

FIG. 5. Vertical temperature profiles with $x^*/L = 3/4$, ↓ configuration, $b/B = 1$.

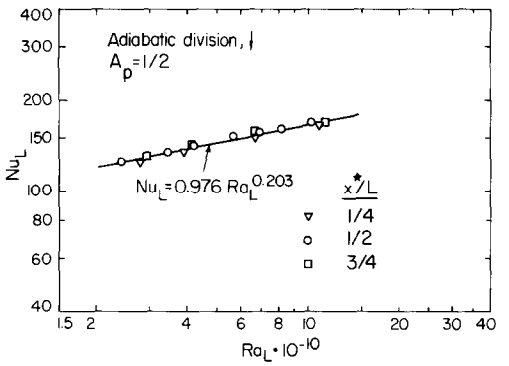

FIG. 6. Heat transfer results for $x^*/L = 1/4$, 1/2, and 3/4, ↓ configuration, $b/B = 1$.

of the separated hot wall boundary layer that was observed in the flow visualization. Further evidence of the presence of this layer is exhibited by the large temperature gradient existing immediately beneath the partial division at $x = x^*$, $y \simeq h$ (for example see Figs. 3–5). Large thermal gradients were not observed in the region $x > x^*$ (to the right of the partition) supporting the flow visualization observation that the separated hot wall boundary layer turns up the cool side of the division with little separation at the lower edge; thereby leaving the core region to the right of the division virtually undisturbed.

The results of the heat transfer measurements for partitions at $x^*/L = 1/4$, 1/2 and 3/4 are summarized in Fig. 6.† It is clear, from Fig. 6, that the transverse position of the partial division has a very small effect on the cross-cavity heat transfer over the parameter range investigated here, i.e. $1/4 \leqslant x^*/L \leqslant 3/4$, $2.25 \times 10^{10} \leqslant Ra_L \leqslant 1.14 \times 10^{11}$. All the data plotted in Fig. 6 fall well within a 5% band around the least squares-generated solid line. However, close inspection of the figure indicates a slight trend toward higher heat transfer rates as x^*/L is increased from 1/4 to 3/4. Thus, cross-cavity heat transfer appears to be only slightly enhanced (all other parameters held fixed) as the partial division is located further from the hot wall and closer to the cold wall. This phenomenon can probably be explained in the following way. Recall that, in general, the peripheral boundary layer flow attains a rather high velocity while traversing the enclosure horizontally, after separating from the hot wall at $y \simeq h$. The velocity of the boundary layer flow is then substantially reduced when reattachment occurs on the cool side of the partition. Hence, it would seem that the mean peripheral boundary layer velocity (i.e. the average over the entire cavity) in the partially divided enclosure can be increased by increasing the value of x^*, i.e. by increasing the horizontal distance between the hot wall and the division. This in turn should increase the overall cross-cavity heat transfer because convective energy transport via the boundary layers is the principal heat transfer mechanism for large Rayleigh number convection. It is possible that there may be a transverse division position (x^*/L near unity) at which the heat transfer will begin to decrease for further increases in x^*/L as the partition approaches the cold wall and begins to interfere with boundary layer entrainment there. This consideration is supported by the calculations of Chang *et al.* [4] where it is shown that heat transfer is decreased as the floor and ceiling divisions of that study are moved close to the heated or the cooled vertical walls. The experiments of Janikowski *et al.* [9] in tall ($A = 5$) air-filled enclosures fitted with ceiling and floor baffles also confirm this expectation. Flow visualization [9] indicates that moving the partitions close to the hot wall on the floor and close to the cold wall on the ceiling limits convection over the lower portion of the hot wall and over the upper portion of the cold wall.

3.2. *Upward-extending partitions*

Flow visualization, temperature measurements, and heat transfer measurements were also carried out for a partition of length, $H/2$, extending upward (↑) from the enclosure floor at the position $x/L = 1/2$, that is, centrally dividing the enclosure.

It can be shown that in the centrally-divided enclosure a symmetry exists between the flows in the ↑ and ↓ configurations. Specifically, for constant fluid properties (excluding the Boussinesq approximation) the governing system of equations and boundary conditions for the ↑ configuration is transformed into the system for the ↓ configuration by means of the transformation

$$x \to L - x, \tag{1}$$

$$y \to H - y, \tag{2}$$

$$u(x, y) \to -u(L-x, H-y), \tag{3}$$

$$v(x, y) \to -v(L-x, H-y), \tag{4}$$

$$T(x, y) \to T_h + T_c - T(L-x, H-y). \tag{5}$$

Hence, the correspondence

$$u_\uparrow(x, y) = -u_\downarrow(L-x, H-y), \tag{6}$$

$$v_\uparrow(x, y) = -v_\downarrow(L-x, H-y), \tag{7}$$

$$T_\uparrow(x, y) = T_h + T_c - T_\downarrow(L-x, H-y), \tag{8}$$

exists between the variables u, v and T in the centrally-divided enclosure in the ↑ and ↓ configurations. From the above it can also be shown that

$$Nu_{L\uparrow} = Nu_{L\downarrow}. \tag{9}$$

For details, see refs. [2, 19]. From equations (6) and (7), streamline patterns in the ↓ and ↑ configurations should be related as shown in Figs. 7(a) and (b), respectively. Dye injection carried out for the two configurations

† The equations in Figs. 6 and 9 differ from the expression for $A_p = 1/2$ given in ref. [1] because different sets of data were used in the correlations. However, the equations give results which deviate from the relation of ref. [1] by less than 3% over the Rayleigh number range, $2 \times 10^{10} \leqslant Ra_L \leqslant 10^{11}$.

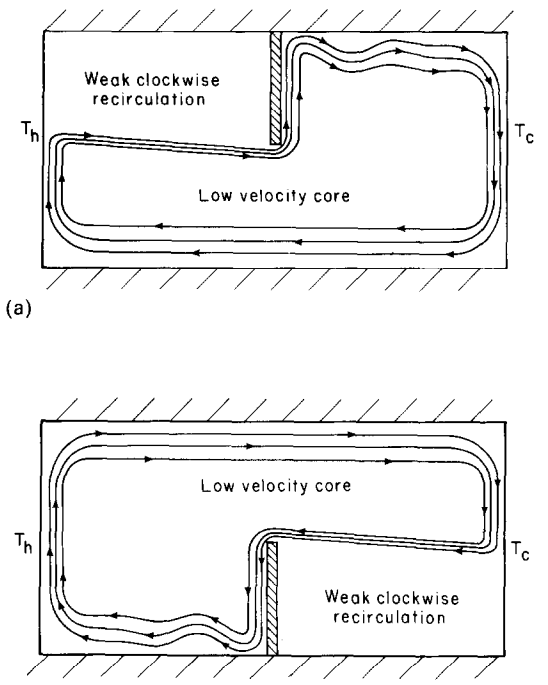

FIG. 7. (a) Flow pattern observed in the ↓ configuration, $Ra_L = O(10^{10})$, $b/B = 1$. (b) Flow pattern observed in the ↑ configuration, $Ra_L = O(10^{10})$, $b/B = 1$.

indicated just this kind of correspondence, i.e. boundary layer separation occurred on the cold wall for the ↑ configuration and the region of weak recirculation was located in the lower right-hand quadrant of the enclosure. Any discrepancy between the experimentally observed patterns and equations (6) and (7) was too subtle to be detected by the qualitative dye visualization technique employed here. According to Winters [2] the experiments of Duxbury [3] with air resulted in flow patterns in the ↑ and ↓ configurations which did not obey the symmetry restrictions (6) and (7). Winters attributes the absence of symmetry in the flow patterns of Duxbury to the significant heat losses ($\sim 40\%$) existing in these experiments.

In nondimensional form, equation (8) can be written as

$$\theta_{\uparrow}(x/L, y/H) = 1 - \theta_{\downarrow}(1 - x/L, 1 - y/H), \qquad (10)$$

where

$$\theta \equiv (T - T_c)/(T_h - T_c).$$

The vertical temperature profiles measured in the ↑ and ↓ enclosure configurations at $x/L = 1/2$ are plotted in Fig. 8. Note that the abscissa of Fig. 8 indicates $\theta_{\uparrow}(x/L, y/H)$ for the ↑ partition configuration and $1 - \theta_{\downarrow}(1 - x/L, 1 - y/H)$ for the ↓ case. If equation (10) was satisfied exactly by the experimental profiles, the two curves in Fig. 8 would coincide. There are two reasons why the observed discrepancy might arise. First, the transformation leading to equation (10) is only valid if thermal boundary conditions in both the ↑ and ↓ configurations are perfect. Note that for the ↓ division the upper left quadrant of the enclosure contains an essentially stagnant body of hot (50–80°C) fluid (cf. Fig. 4), thus inviting heat losses to the lower temperature ambient through the imperfect ceiling insulation. In the equivalent region for the ↑ case (lower right quadrant), the fluid is roughly at the same temperature as the ambient (23–28°C) and hence losses through the floor should be small. Hence, the *degree* of imperfection in the thermal conditions on the horizontal boundaries is quite different for ↑ and ↓ partial divisions. Secondly, equation (10) is only valid when fluid thermal and transport properties are constant, independent of temperature. The smallest value of $(T_h - T_c)$ in the present experiments was 24°C. Hence fluid properties varied substantially throughout the enclosure.

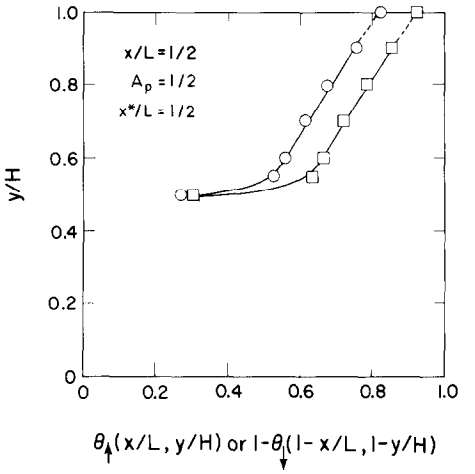

FIG. 8. Vertical temperature profiles for the ↑ and ↓ enclosure configurations:
$x/L = 1/2$, $b/B = 1$. □ = $\theta_{\uparrow}(x/L, y/H)$, $Ra_L = 2.25 \times 10^{10}$.
○ = $1 - \theta_{\downarrow}(1 - x/L, 1 - y/H)$, $Ra_L = 4.17 \times 10^{10}$.

The effect of variable fluid properties and imperfect thermal boundary conditions on the correspondence of the heat transfer with equation (9) is very small as may be observed from Fig. 9 which shows the measured

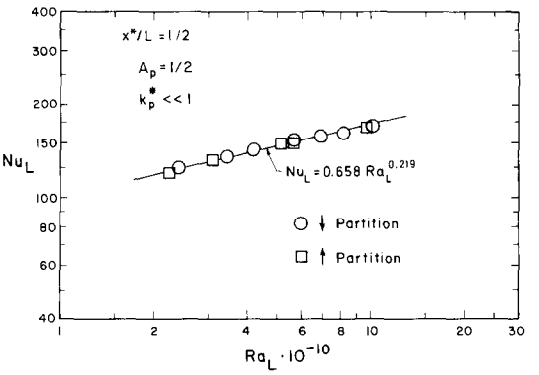

FIG. 9. Heat transfer results for the ↑ and ↓ configurations, $x^*/L = 1/2$, $b/B = 1$.

Nusselt number for both the ↑ and ↓ configurations. It is noted that the heat transfer data of Duxbury [3], obtained using air, also obey equation (9) quite well. The variable property calculations of Leonardi and Reizes [20] for a gas enclosed in an undivided cavity show that when $(T_h - T_c)/T_r = 0.4$ the heat transfer is changed only about 5% from the constant property, Boussinesq value for $Ra_L = 5 \times 10^5$. The present experiments were confined to the range, $0.08 < (T_h - T_c)/T_r < 0.18$. Perhaps the apparent insensitivity of the Nusselt number to property variations and imperfections in the boundary conditions can be attributed to the integral nature of the average heat transfer.

4. THREE-DIMENSIONAL PARTITIONS: RESULTS AND DISCUSSION

4.1. *Flow visualization*

The flow observed in the enclosure with the 3-D partition was complex. Dye injection at the point $x = L$, $y = H$, $z = B/2$ confirmed the expected downflow in the cold boundary layer adjacent to the cold wall and the horizontal flow across the enclosure floor in a manner similar to that observed in the experiments with the 2-D partition. The stream of dye remained coherent in the plane $z = B/2$ until reaching a point very near the hot wall on the floor ($y = 0$). There the dye stream divided into three separate streams. The largest stream remained in the plane $z = B/2$ while the other two moved symmetrically away from this plane in the $+z$ and $-z$ directions. These latter two streams of dye exhibited the strongly 3-D nature of the flow, including a swirling motion in which the dye was first carried away from the plane $z = B/2$ along the upper part of the hot wall and then back toward the plane $z = B/2$ along the partition. Details of this 3-D flow away from and towards the plane $z = B/2$ were difficult to discern because observations could only be made normal to the x–y plane. Hence the following discussion of the flow visualization will be confined to the streamlines which remained in the $z/B = 1/2$ plane.

The flow in the plane $z/B = 1/2$ in the 3-D configuration exhibited a number of similarities with the 2-D cases discussed in Section 3 and in ref. [1]. This includes the strong peripheral boundary layer flow, boundary layer separation at $y \simeq h$ on the hot wall, and reattachment at the lower edge of the soffit. However, the flow in the plane $z/B = 1/2$ in the 3-D geometry with $h/H < 1$, i.e. with a soffit present, did exhibit a number of different features including a high degree of Rayleigh number dependence, intense turbulence, new regions of boundary layer separation, and a strong boundary layer–enclosure core interaction.

Figure 10 depicts the flow pattern in the enclosure with the 3-D partition ($b/B = 0.093$) in the plane $z = B/2$ with $h/H = 1$; i.e. the case of the rectangular opening extending all the way (from the floor) to ceiling so that no soffit is present. In this case the flow in the plane $z = B/2$ is qualitatively very much like that in the undivided 2-D enclosure (i.e. $b/B = 1$) [1] with the exception that the fluid in the horizontal layers near the enclosure floor and the ceiling have a substantially greater velocity in the 3-D geometry than in the corresponding 2-D case.

The phenomena observed when a soffit was present are shown in Figs. 11 and 12. These figures show the flow in the plane $z = B/2$ for the 3-D geometry with $h/H = 3/4$ at Rayleigh numbers of 3×10^{10} and 10^{11}, respectively. Comparison of Figs. 11 and 12 indicates that when a soffit is present the flow field is very sensitive to Ra_L. At the lower value Rayleigh number (3×10^{10}), cf. Fig. 11, the peripheral boundary layer flow remains everywhere laminar, as in the 2-D case [1]. However, there are now two new regions of boundary layer separation present. The separated hot wall boundary layer attaches to the lower edge of the soffit but then immediately separates from the cool side of the soffit, thickening slightly before attachment occurs on the enclosure ceiling. There is another point of boundary layer separation downstream of this reattachment point, toward the top of the cold wall, where a small region of weak laminar eddying motion was observed, cf. Fig. 11.

At the higher value Rayleigh number ($Ra_L = 10^{11}$) for the same value of h/H, cf. Fig. 12, the flow was quite

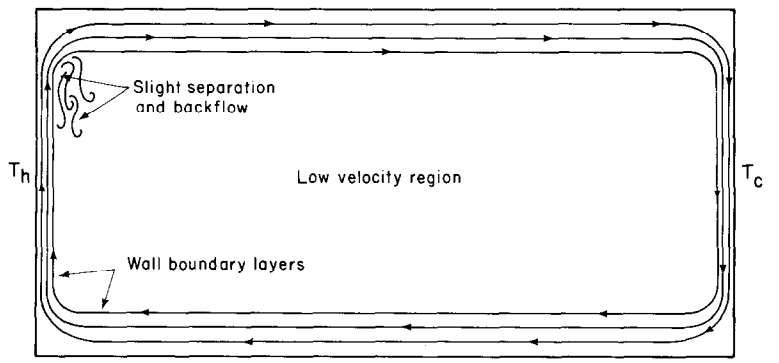

FIG. 10. Flow pattern observed in the plane $z = B/2$, with $h/H = 1$, $Ra_L = 3 \times 10^{10}$, $b/B = 0.093$.

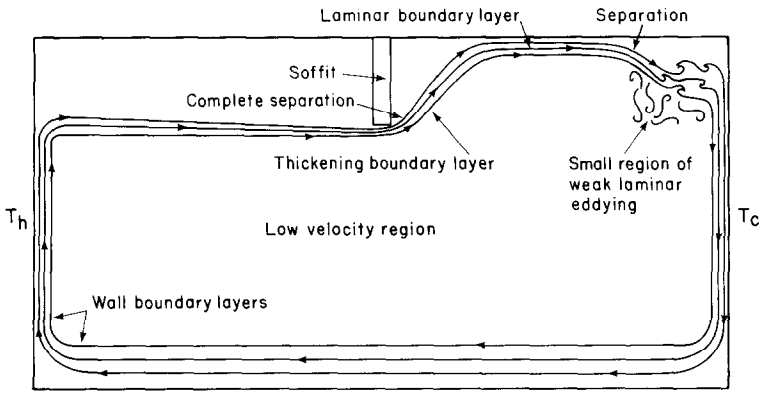

FIG. 11. Flow pattern observed in the plane $z = B/2$, with $h/H = 3/4$, $Ra_L = 3 \times 10^{10}$, $b/B = 0.093$.

different. At $Ra_L = 10^{11}$ very little separation of the boundary layer occurred at the lower edge of the soffit, the flow turning sharply upward along the cool side of the partition, with small laminar vortices being shed at regular intervals from the lower edge of the soffit. At the intersection of the partition and the ceiling, the layer undergoes an almost immediate transition to an intensely turbulent flow. It was easy to distinguish between regions of laminar and turbulent flow due to the fluctuating index of refraction field in the turbulent regions resulting from the fluctuating temperature field there. The fluctuations were visually evident due to the resulting shadowgraph effect as light rays passed through the enclosure in the $-z$-direction and were incident on the white backdrop at the opposite endwall. The extent of the turbulent regions in the cavity could also be determined by observing where the laminar dye filaments broke down into highly chaotic, turbulent motion. Slightly downstream of the separation region on the ceiling, the intensity of the turbulence rapidly decayed as the fine-scale structure of the turbulence gave way to a much larger scale eddying motion. The flow relaminarized upon reattaching to the upper section of the cooled vertical wall. Note that within the region $x \gtrsim L/2$, $y \gtrsim h$, there was a section of the enclosure core which was interacting with the turbulent layer just above it, cf. Fig. 12. The core flow remained laminar in this region, although filaments of dye could be seen as they were ejected downward from the turbulent ceiling layer, creating large eddies which penetrated roughly to the elevation of the lower edge of the soffit, $y \simeq h$. This interior core–turbulent boundary layer interaction is reminiscent of the interactions observed by Elder [21] in his experiments with water in undivided enclosures of large aspect ratio, $10 \leqslant A \leqslant 30$.

The fundamental aspects of the flow in the experiments with $h/H = 1/2$ and $1/4$ were qualitatively the same as in the $h/H = 3/4$ case with the exception of two features. Separation of the laminar boundary layer at low Rayleigh number ($\sim 10^{10}$) from the soffit, on the cool side, was less severe for $h/H = 1/2$ and $1/4$ than for the case $h/H = 3/4$. For $h/H = 1/4$ only a very small separation zone was observed at the extreme lower edge of the soffit. Also, it was discovered that for $h/H = 1/2$ separation of the boundary layer from the ceiling in the cold zone of the enclosure occurred nearer to the partition, i.e. separation occurred roughly at the position $x = 3L/4$ for the case $h/H = 1/2$.

It appears, from the previous discussion, that the

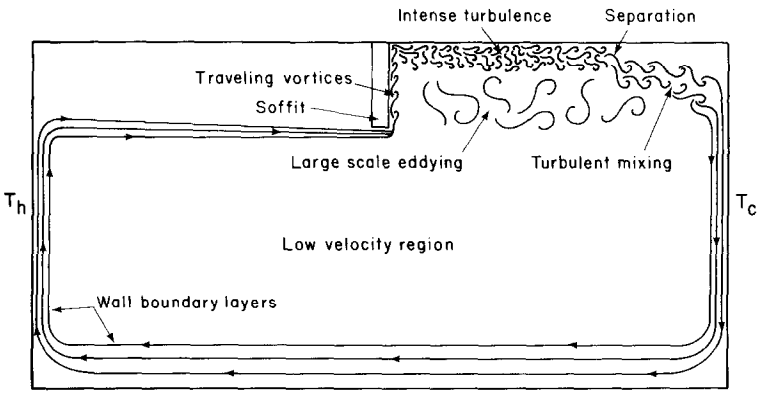

FIG. 12. Flow pattern observed in the plane $z = B/2$, with $h/H = 3/4$, $Ra_L = 10^{11}$, $b/B = 0.093$.

presence of a soffit ($h < H$) in the 3-D enclosure ($b < B$) has a profound effect on the enclosure flow at large Rayleigh number. This is in contrast to the relatively uneventful pattern observed for $h/H = 1$ (i.e. no soffit) in Fig. 10. However, it is apparently *the existence of the soffit coupled with the 3-D geometry and not the presence of the soffit alone* which gives rise to the local regions of turbulent flow in Fig. 12. This is because the 2-D soffit; that is, the partition with $b = B$, discussed in Section 3 and in ref. [1], resulted invariably in laminar flow. In the 3-D case, variations in the height of the rectangular opening cause substantial changes in the flow. In addition, changes of less than one order of magnitude in the Rayleigh number, for a given size opening (b and h fixed), caused radical changes in the flow. Apparently, the greatly diminished area available for flow from the hot to the cold zone of the enclosure and vice versa results in greater velocities through the aperture. This, coupled with instabilities introduced into the flow by the soffit may result in the increased sensitivity of the flow to the Rayleigh number. Note that this trend is opposite to that observed in the 2-D enclosure, where partitions were found to have a stabilizing effect on the laminar flow [1]. However, in the 2-D case the instabilities noted were in the boundary layers on the vertical heated and cooled surfaces, while in the 3-D enclosure they are largely confined to the region, $x \geqslant L/2$, $y \geqslant h$, near the symmetry plane, $z = B/2$.

4.2. *Heat transfer*

Heat transfer measurements were made in the water-filled, 3-D enclosure for rectangular opening heights, $h = H$ (no soffit), $3H/4$, $H/2$ and $H/4$, for an opening width, $b = 0.093B$. Table 1 shows the heat transfer results obtained for $h/H = 1/2$ while the heat transfer data for the cases $h/H = 1$, 3/4, 1/2, and 1/4 are plotted in Fig. 13. A three-parameter power law correlation for all the measurements for the 3-D enclosure resulted in the relation

$$Nu_L = 1.19(h/H)^{0.401}\, Ra_L^{0.207} \begin{cases} 1/4 \leqslant h/H \leqslant 1, \\ b/B = 0.093, \end{cases} \quad (11)$$

with a root mean square deviation from the data of about 4. This relation is plotted in Fig. 13 (solid curve) along with the equation

$$Nu_L = 0.762(h/H)^{0.473} Ra_L^{0.226} \begin{cases} 1/4 \leqslant h/H \leqslant 1, \\ b/B = 1, \end{cases} \quad (12)$$

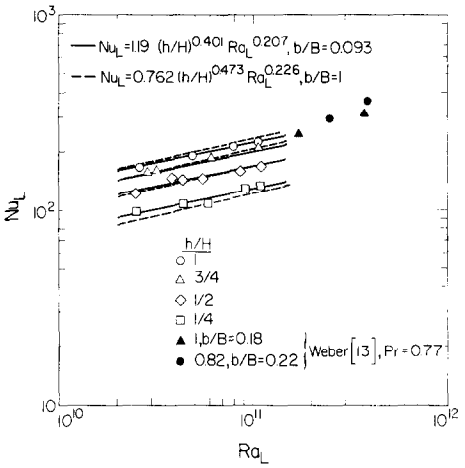

FIG. 13. Heat transfer results for the 3-D configuration, $1/4 \leqslant h/H \leqslant 1$, $b/B = 0.093$.

(dashed curve) which was obtained from the experiments of ref. [1] for an enclosure partially divided by a 2-D division ($b = B$) for $h/H = 1, 3/4, 1/2$ and $1/4$. It is somewhat surprising that at each value of h/H there is relatively little difference in the cross-cavity heat transfer between the 2- and 3-D cases. For the cases $h/H = 1$ and 3/4, heat transfer in the 2-D geometry exceeds the heat transfer in the 3-D case by less than about 5% while for the cases $h/H = 1/2$ and $1/4$ the heat transfer in the 3-D geometry exceeds that in the 2-D case by 5–10%. However, recall that the 3-D enclosure configuration results in regions of intense turbulence and strong interaction between the turbulent boundary layer and the enclosure core, neither of which were observed in the 2-D experiments of ref. [1] at the same values of the Rayleigh number. Hence, it is not too surprising that the cross-cavity heat transfer in the 3-D geometry may be smaller or even slightly larger than in the 2-D configuration because the flow may be drastically different. The apparent lack of heat transfer dependence on the opening width parameter, b/B, observed here, was also observed in the experiments of Weber [13] with Freon-12 vapor ($Pr = 0.77$) in an enclosure of similar geometry. In Weber's experiment, the rectangular opening width was varied over the range, $0.07 \leqslant b/B \leqslant 0.40$, and it was found that

$$Nu_L \sim (b/B)^{0.13}, \quad (13)$$

a rather weak dependence.

Table 1. Heat transfer data, $h/H = 1/2$, $b/B = 0.093$

Run	Ra_L	Pr	Nu_L	Q_h (W)	Q_c (W)	$(Q_h - Q_c)/Q_h$ (%)	T_h (°C)	T_c (°C)	$(T_h - T_c)$ (°C)
1	5.50×10^{10}	3.6	144	1620	1500	7.4	69.0	28.9	40.1
2	8.49×10^{10}	3.2	158	2240	2160	3.6	80.9	29.8	51.1
3	3.88×10^{10}	3.9	141	1230	1150	6.5	61.3	29.7	31.6
4	1.09×10^{11}	3.0	167	2790	2610	6.4	88.5	29.5	59.0
5	2.45×10^{10}	4.3	122	806	755	6.3	51.9	27.7	24.2
6	4.34×10^{10}	3.7	144	1330	1230	7.5	64.2	31.2	33.0

Figure 13 also includes data from Weber's experiments corresponding to the cases, $h/H = 1$, $b/B = 0.18$, and $h/H = 0.82$, $b/B = 0.22$, for Rayleigh numbers between 1.7×10^{11} and 3.9×10^{11}. The major differences between the present experiments and those of Weber are geometrical. Weber's enclosure had an aspect ratio, $A = H/L = 0.3$ and a breadth aspect ratio, $B/L = 0.5$ rather than the values $H/L = 1/2$ and $B/L = 2.7$ for the present apparatus. Despite these differences in geometry, including the different opening width, b, and the difference in Prandtl number, Weber's data for $h/H = 1$ (no soffit) agree rather well with the present results for $h/H = 1$. Note, however, that Weber's data for $h/H = 0.82$ fall *above* his data for $h/H = 1$ and agree less favorably with the present data (cf. Fig. 13). It was found in the present experiments that heat transfer always decreased with decreasing h/H, although an increase in heat transfer with decreased h/H is conceivable if the presence of the soffit causes a sufficiently large change in the enclosure flow regime. This question was not addressed by Weber [13].

5. CONCLUSIONS AND RECOMMENDATIONS

It was found that the basic flow pattern observed in the centrally-divided 2-D enclosure in ref. [1] persists even when the partition is moved transversely within the range $1/4 \leqslant x^*/L \leqslant 3/4$. The three distinct flow regions merely change shape to accommodate the changing position of the partition. Similarly, it was shown that the temperature field remains qualitatively unaltered by changes in the location of the partition. Also, the cross-cavity heat transfer was shown to be only slightly dependent on the partition location within the range of x^* investigated. Experiments with $\uparrow$ and $\downarrow$ configurations indicated that the flow and overall heat transfer follow the theoretical symmetry laws rather well while the temperature field obeys the symmetry restrictions in a qualitative way only. The deviation of the measured temperature from the theoretical symmetry law is attributed to varying fluid properties and imperfections in the thermal boundary conditions that were present in the experiments.

It is found that the flow pattern in the 3-D enclosure, when a soffit is present ($h < H$), is very much different from the pattern observed in the 2-D enclosure. For the 3-D configuration, the flow at the enclosure midplane, $z = B/2$, resembles the flow in the 2-D case only when no soffit is present, i.e. when $h/H = 1$. The presence of a soffit ($h/H < 1$) has a substantial effect on the flow in the 3-D enclosure causing regions of localized turbulence, instability, boundary layer separation and reattachment, and a high degree of Rayleigh number dependence. While the presence of a 2-D soffit has a stabilizing effect on the enclosure flow, a 3-D soffit clearly has a destabilizing effect for Rayleigh numbers approaching 10^{11}. The cross-cavity heat transfer, however, appears to be rather insensitive to the width of the rectangular opening in the 3-D partition; little difference was observed in the heat transfer between the 2-D experiments of ref. [1] and the present 3-D experiments, for the same values of h/H. This finding is in accord with the observation of Weber [13] for Freon-filled enclosures at similar values of the Rayleigh number.

For the 3-D case, the effect of partition location with respect to the heated and cooled vertical walls and the effect of the location of the opening in the partition have not been addressed. In addition, the effect of partition thickness on the cross-cavity heat transfer, which was found to be significant by Brown and Solvason [12], was not considered in the present work. It is recommended that these effects be examined in future studies on convection in enclosures with partitions.

Acknowledgements—This work has been supported in part by the Research and Development Branch, Passive and Hybrid Division of the Office of Solar Applications for Buildings, U.S. Department of Energy, under Contract No. W-7405-ENG-48. The authors also wish to acknowledge Fred Bauman of the Lawrence Berkeley Laboratory for his assistance during the early stages of this research.

REFERENCES

1. M. W. Nansteel and R. Greif, Natural convection in undivided and partially divided rectangular enclosures, *J. Heat Transfer* **103,** 623–629 (1981).
2. K. H. Winters, The effect of conducting divisions on the natural convection of air in a rectangular cavity with heated side walls, *Proc. 3rd Joint AIAA/ASME Thermophysics, Fluids, Plasma and Heat Transfer Conf.*, St. Louis (1982).
3. D. Duxbury, An interferometric study of natural convection in enclosed plane air layers with complete and partial central vertical divisions, Ph.D. thesis, University of Salford, U.K. (1979).
4. L. C. Chang, J. R. Lloyd and K. T. Yang, A finite difference study of natural convection in complex enclosures, *Proc. 7th Int. Heat Transfer Conf.*, Munich, Federal Republic of Germany, pp. 183–188 (1982).
5. N. N. Lin and A. Bejan, Natural convection in a partially divided enclosure, personal communication (1983).
6. F. Bauman, A Gadgil, R. Kammerud and R. Greif, Buoyancy driven convection in rectangular enclosures: experimental results and numerical calculations, ASME 80-HT-66 (1980).
7. N. P. Lynch and J. R. Lloyd, An experimental investigation of the transient build-up of fire in a room-corridor geometry, *Proc. 18th Int. Symp. on Combustion*, The Combustion Institute, Pittsburgh, Pennsylvania (1980).
8. A. C. Ku, M. L. Doria and J. R. Lloyd, Numerical modeling of unsteady buoyant flows generated by fire in a corridor, *Proc. 16th Int. Symp. on Combustion*, The Combustion Institute, Pittsburgh, Pennsylvania, pp. 1373–1384 (1976).
9. H. E. Janikowski, J. Ward and S. D. Probert, Free convection in vertical air-filled rectangular cavities fitted with baffles, *Proc. 6th Int. Heat Tranfer Conf.*, Vol. 2, pp. 257–262 (1978).
10. A. F. Emery, Exploratory studies of free convection heat transfer through an enclosed vertical liquid layer with a vertical baffle, *J. Heat Transfer* **91,** 163–165 (1969).
11. P. Chao, Effects of non-uniform heating and internal baffles on natural convection in inclined rectangular enclosures, Ph.D. thesis, Department of Chemical Engineering, University of Pennsylvania, Philadelphia, Pennsylvania (1981).

12. W. G. Brown and K. R. Solvason, Natural convection heat transfer through rectangular openings in partitions—I, *Int. J. Heat Mass Transfer* **5**, 859–868 (1962).
13. D. D. Weber, Similitude modeling of natural convection heat transfer through an aperture in passive solar heated buildings, Ph.D. thesis, Department of Physics, University of Idaho, Moscow, Idaho (1980).
14. I. Catton, P. S. Ayyaswamy and R. M. Clever, Natural convection flow in a finite, rectangular slot arbitrarily oriented with respect to the gravity vector, *Int. J. Heat Mass Transfer* **17**, 173–184 (1974).
15. E. I. Lee and V. Sernas, Numerical study of heat transfer in rectangular air enclosures of aspect ratio less than one, ASME 80-WA/HT-45 (1980).
16. K. H. Winters, Personal communication (1982).
17. R. Rubel and F. Landis, Numerical study of natural convection in a vertical rectangular enclosure, *Physics Fluids Supp. II* **12**, 203–213 (1969).
18. E. R. G. Eckert and W. D. Carlson, Natural convection in an air layer enclosed between two vertical plates with different temperatures, *Int. J. Heat Mass Transfer* **2**, 106–120 (1961).
19. M. W. Nansteel, Natural convection in enclosures, Ph.D. thesis, Department of Mechanical Engineering, University of California, Berkeley, California (1982).
20. E. Leonardi and J. A. Reizes, Natural convection in compressible fluids with variable properties, *Proc. 1st Int. Conf. on Numerical Methods in Thermal Problems*, Swansea, U.K., pp. 297–306 (1979).
21. J. W. Elder, Turbulent free convection in a vertical slot, *J. Fluid Mech.* **23**, 99–111 (1965).

ETUDE DE LA CONVECTION NATURELLE DANS DES CAVITES AVEC DES PARTITIONS BI-OU-TRIDIMENSIONNELLES

Résumé—On étudie expérimentalement le transfert thermique et l'écoulement dans une cavité rectangulaire avec une partition verticale adiabatique. La cloison est orientée parallèlement aux deux parois verticales isothermes, l'une d'elles étant chaude et l'autre froide, tandis que toutes les autres surfaces de la cavité sont isolées. Les expériences sont faites avec l'eau pour des nombres de Rayleigh de 10^{10}–10^{11} et un rapport de forme (hauteur/largeur) d'un demi. Les températures du fluide sont obtenues avec des thermocouples et le transfert thermique à travers la cavité est obtenu en fonction du nombre de Rayleigh et de la géométrie de la partition. L'écoulement est visualisé par injection colorée. Deux cas sont étudiés. Dans le premier, la partition est de hauteur constante sur toute la largeur de la cavité pour réaliser une géométrie bidimensionnelle. On examine l'effet de la position transversale et de l'extension vers le haut ou vers le bas (orientation) de la division. Dans le second cas, la partition divise complètement la cavité sauf pour une ouverture rectangulaire qui permet à la convection de passer à travers la cavité. On étudie la dépendance de l'écoulement et du transfert thermique de cavité vis-à-vis du nombre de Rayleigh et de la taille de l'ouverture dans la partition.

EINE UNTERSUCHUNG DER FREIEN KONVEKTION IN HOHLRÄUMEN MIT ZWEI- UND DREIDIMENSIONALEN UNTERTEILUNGEN

Zusammenfassung—Es wurden der Wärmeübergang und die Strömung in einem rechteckigen Hohlraum, der mit einer adiabaten Trennwand versehen war, experimentell untersucht. Die Trennwand ist parallel zu den zwei vertikalen isothermen Wänden orientiert, von denen die eine beheizt und die andere gekühlt ist, während alle anderen Flächen des Hohlraums isoliert sind. Die Experimente wurden mit Wasser bei Rayleigh-Zahlen im Bereich von 10^{10}–10^{11} und einem Seitenverhältnis (Höhe zur Breite) von 0,5 durchgeführt. Die Flüssigkeitstemperaturen wurden mit Thermoelementen gemessen. Die Wärmeübertragung quer durch den Hohlraum erhält man als eine Funktion der Rayleigh-Zahl und der Aufteilungsgeometrie. Die Strömung wurde mit Farbstoffinjektion sichtbar gemacht. Zwei Fälle wurden untersucht. Im ersten Fall hat die Trennwand konstante Höhe über die gesamte Breite des Hohlraums, was zu einer zweidimensionalen Geometrie führt. Hier wurde der Einfluß der Queranordnung, der Unterteilung und ihrer Ausdehnung nach oben oder unten untersucht. Im zweiten Fall unterteilte die Trennwand den Hohlraum vollständig, bis auf eine rechteckige Öffnung, welche freie Konvektion quer durch den Hohlraum erlaubte. Die Abhängigkeit der Strömung und der Wärmeübertragung quer durch den Hohlraum von der Rayleigh-Zahl und der Größe der Öffnung in der Trennwand wurden in diesem Fall untersucht.

ИССЛЕДОВАНИЕ ЕСТЕСТВЕННОЙ КОНВЕКЦИИ В ЗАМКНУТЫХ ПОЛОСТЯХ С ДВУХМЕРНЫМИ И ТРЕХМЕРНЫМИ ПЕРЕГОРОДКАМИ

Аннотация—Проведено экспериментальное исследование теплопереноса и течения жидкости в прямоугольной замкнутой полости с вертикальной адиабатической перегородкой. Перегородка ориентирована параллельно двум вертикальным изотермическим стенкам, одна из которых нагревается, а вторая охлаждается. Остальные поверхности полости теплоизолированы. Эксперименты проводились с водой при числах Релея в диапазоне 10^{10}–10^{11} и отношении высоты к ширине полости, равном 1/2. Температура жидкости определялась с помощью термопар, а теплоперенос через полость определялся как функция числа Релея и геометрии перегородки. Визуализация потока осуществлялась с помощью краски. Проведено исследование двух случаев. В первом перегородка была одинаковой высоты по всей ширине полости, что соответствует двумерной геометрии. Исследовалось влияние положения перегородки и ее ориентации. Во втором случае перегородка полностью делила полость, но имела прямоугольный вырез, через который происходило течение поперек полости. Исследовалась зависимость течения и теплопереноса через полость от числа Релея и размера отверстия в перегородке.